MR Lymphangiography in Children: Technique and Potential Applications[1]

Govind B. Chavhan, MD, DABR
Joao G. Amaral, MD
Michael Temple, MD
Maxim Itkin, MD

Abbreviations: CCL = central conducting lymphatic, DCE = dynamic contrast-enhanced, GBCM = gadolinium-based contrast material, MIP = maximum intensity projection, PLPS = pulmonary lymphatic perfusion syndrome, 3D = three-dimensional

RadioGraphics 2017; 37:1775–1790

https://doi.org/10.1148/rg.2017170014

Content Codes: MR PD

[1]From the Department of Diagnostic Imaging (G.B.C., J.G.A., M.T.) and Division of Image Guided Therapy, Department of Diagnostic Imaging (J.G.A., M.T.), The Hospital for Sick Children, Medical Imaging, University of Toronto, 555 University Ave, Toronto, ON, Canada M5G 1X8; and Center for Lymphatic Imaging and Interventions, Children's Hospital of Philadelphia, Hospital of the University of Pennsylvania, Philadelphia, Pa (M.I.). Received February 17, 2017; revision requested May 2 and received June 4; accepted June 13. For this journal-based SA-CME activity, the authors, editor, and reviewers have disclosed no relevant relationships. **Address correspondence to** G.B.C. (e-mail: *drgovindchavhan@yahoo.com*).

SA-CME LEARNING OBJECTIVES

After completing this journal-based SA-CME activity, participants will be able to:

■ Discuss the anatomy of the lymphatic system.

■ List imaging methods used in assessment of the lymphatic system in children.

■ Describe the technique of MR lymphangiography and its applications in children.

See www.rsna.org/education/search/RG.

The lymphatic system, an important component of the circulatory system with essential physiologic functions, can be affected by various disease processes. There has been a delay in the development of effective imaging methods for the lymphatic system due to its small size, which limits visualization as well as introduction of contrast material. Traditionally, the lymphatic system has been imaged by injecting contrast material or radiotracers into the feet or hands. This is not sufficient for assessment of the central conducting lymphatics (CCLs) (such as the thoracic duct or the cisterna chyli). Fluoroscopic intranodal lymphangiography with injection of oil-based contrast material into groin lymph nodes improves visualization of CCLs but is limited in practice owing to the use of radiation and the potential risk for paradoxical embolization in children with left-to-right shunt. Dynamic contrast material–enhanced (DCE) magnetic resonance (MR) lymphangiography, which is performed by injecting gadolinium-based contrast material into groin lymph nodes, overcomes these limitations. T2-weighted imaging plays a complementary role to DCE MR lymphangiography in the assessment of CCLs. DCE MR lymphangiography demonstrates preserved integrity or any abnormality of the CCLs (including blockage or leak). The technique has recently been used in evaluating pulmonary lymphatic perfusion syndrome in children with plastic bronchitis, neonatal lymphatic flow disorders, and nontraumatic chylothorax. It is useful in identification of the source of chylous ascites and contributes to understanding of the anatomy of lymphatic malformations. It is successfully used for planning of embolization of aberrant lymphatic channels in a variety of lymphatic flow disorders. This review discusses the anatomy and function of the lymphatic system, the evolution of imaging of the lymphatic system, and DCE MR lymphangiography technique and its applications in children.

Introduction

The lymphatic system is an essential component of the circulatory system. It has several important physiologic functions. It is affected by various disease processes, and many conditions have abnormalities of the lymphatic system as their basis. Most of the lymphatic system is composed of a network of vessels that are small, except for main ducts such as the thoracic duct or the cisterna chyli. Over the last half of the 20th century, there was tremendous progress in imaging almost every

TEACHING POINTS

- The lymphatic vessels that come from the right side of the head and neck, right upper extremity, and right side of the chest, lung, and heart drain into the right lymphatic duct. The right lymphatic duct is short (1.25 cm) and opens directly into the venous system at the junction of the right subclavian and right internal jugular veins. Lymph from the rest of the body, including the lower extremities, abdomen (including the liver and intestine), left upper extremity, and left side of the chest, head, and neck, is drained by the thoracic duct.
- Recently, ultrasonography (US)-guided intranodal injection of oil-based contrast material (similar to US-guided intranodal gadolinium injection, explained later) with imaging of CCLs at fluoroscopy has been refined for use in children and successfully used for subsequent lymphatic intervention. This technique provides excellent spatial resolution. Limitations of this technique include exposure to ionizing radiation, longer examination time, limited dynamic information, and limited information about the relationship of lymphatic ducts with surrounding structures. Moreover, oil-based contrast material must be used with caution in children with right-to-left shunts from congenital heart disease or from large pulmonary arteriovenous malformations because of the risk for systemic embolism. Cerebral ethiodized oil embolism after lymphatic embolization has been reported in a child with congenital heart disease and plastic bronchitis, due to direct connection between the lymphatics and the pulmonary venous branch.
- Dynamic postcontrast imaging of the initial movement of contrast material after injection (first passage of contrast material) through the ducts is performed by using T1-weighted 3D gradient sequences such as THRIVE/VIBE/LAVA in the coronal plane that can be acquired in 15–30 seconds. First, a mask image is acquired that is used for subtraction. Then, from the start of intranodal contrast material injection, images are acquired every minute until the contrast material reaches the venous angle where the thoracic duct drains. More frequent imaging (every 30 seconds) can be performed if there is chylolymphatic reflux, defined as passage of contrast agent from the CCLs into lymphatic ducts away from the expected direction of flow. Images in the axial plane can be acquired as required to assess the ducts. Washout of contrast agent from normal lymphatic ducts typically occurs in 15–30 minutes.
- After the start of intranodal injection, contrast material typically appears in the retroperitoneal lymphatics at the aortic bifurcation and along the iliac ducts within 2 minutes. A normal cisterna chyli is opacified in 3–6 minutes. Thereafter, the passage of contrast material superiorly from the cisterna chyli is rapid and reaches the venous angle through the thoracic duct approximately in the next 2–3 minutes. Contrast material is typically washed out from the normal CCL in 15–20 minutes and is accompanied by renal enhancement and excretion.
- In patients with total cavopulmonary connection, the prevalence of plastic bronchitis is approximately 4%. PLPS serves as an anatomic substrate for the condition. Elevated central venous pressure in these patients results in increased production of lymph as well as an increase in impedance to lymphatic drainage. This results in congestion in the central lymphatic system and in PLPS can result in overflow of lymph into the lung parenchyma. This abnormal lymphatic flow into the lungs causes protein leakage into the airways and cast formation. Dilatation of subpleural and interlobular lymphatics has been shown in patients with plastic bronchitis and intestinal lymphangiectasia in patients with protein-losing enteropathy demonstrated at pathologic analysis.

system in the human body. However, imaging of the lymphatic system trailed behind, primarily because of difficulties in introduction of contrast material into the lymphatic ducts. Until recently, there were only two methods of contrast material–enhanced lymphatic imaging: direct cannulation of the lymphatic ducts (pedal lymphangiography) and interstitial injection of contrast agents that are absorbed into the lymphatic system (lymphoscintigraphy and lower extremity magnetic resonance [MR] lymphangiography). Unfortunately, neither technique can be used to reliably image the central lymphatic system. Recent advances in lymphatic imaging technology as well as successful development of newer lymphatic interventional techniques have prompted progress in imaging of the central lymphatic system (1–4). One such recently developed technique is dynamic contrast-enhanced (DCE) MR lymphangiography, which is being increasingly used in clinical practice (4,5). Similar advances have occurred in imaging of the lymphatic system of the upper and lower extremities.

This review focuses on imaging of the central conducting lymphatics (CCLs). Peripheral lymphangiography is not discussed. We discuss the anatomy and function of the lymphatic system, progress in imaging of the lymphatic system, and DCE MR lymphangiography technique for CCLs, with current and potential applications in children.

Anatomy and Function of the Lymphatic System

Lymph is a bodily fluid that originates in the interstitial tissues. Lymph is excess of tissue fluid derived from blood plasma and removed by the lymphatic system. Lymph contains oxygen, nutrients, hormones, fatty acids, toxins, and cellular waste products.

The lymphatic system consists of a network of small terminal lymphatic ducts, which collect lymph from tissues, and larger lymphatic ducts conducting lymph from terminal lymphatics to veins, with lymph nodes interspersed in the lymphatic pathways (6). Terminal lymphatics are small lymphatic vessels originating in tissues of the body. The lymphatic ducts contain valves, similar to those for veins, for unidirectional lymphatic flow from tissues and organs into the systemic venous system. Lymph enters the lymph nodes via afferent lymphatic ducts and leaves via efferent lymphatic ducts. Lymph nodes regulate the composition of the lymph and mount immune responses if pathogens are detected.

The lymphatic vessels can be divided into three types depending on their origin: soft-tissue, liver, and intestinal lymphatic ducts (7).

The lymphatic vessels that come from the right side of the head and neck, right upper extremity,

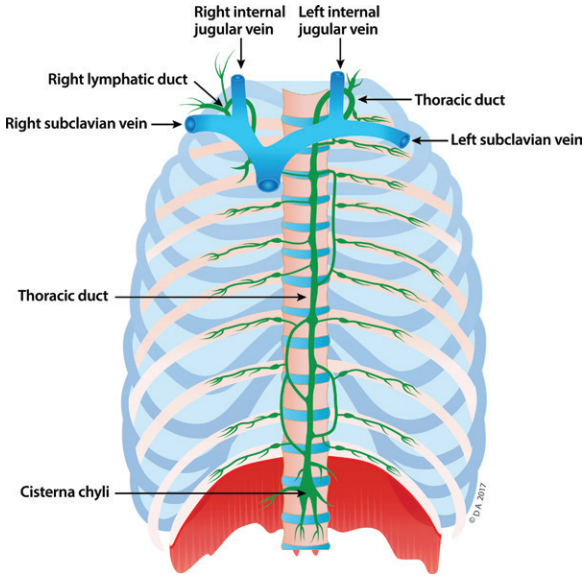

Figure 1. Diagram illustrates the normal anatomy of the lymphatic system.

and right side of the chest, lung, and heart drain into the right lymphatic duct. The right lymphatic duct is short (1.25 cm) and opens directly into the venous system at the junction of the right subclavian and right internal jugular veins (6). Lymph from the rest of the body, including the lower extremities, abdomen (including the liver and intestine), left upper extremity, and left side of the chest, head, and neck, is drained by the thoracic duct (Fig 1). In its classic description, the thoracic duct is a long channel, measuring approximately 38–45 cm in adults. It typically enters the venous system at the left venous angle, which is formed by the junction of the left subclavian and internal jugular veins. It starts as a triangular or saccular dilatation (the cisterna chyli) over the first or second lumbar vertebral body and runs to the right of the aorta over the spine. At approximately the fifth thoracic vertebral body, it crosses over to the left side in the superior mediastinum and ultimately runs to the left side of the neck. However, the anatomy of the thoracic duct can be variable because of the complexities of embryologic development. The cisterna chyli can have a variety of shapes, including an inverted Y, an inverted V, or a string of pearls (8). The cisterna chyli measures approximately 5–20 mm in width and 5–7 cm in craniocaudal dimension in adults; its caliber may change with contraction (8). The thoracic duct transports approximately 1.5–2.5 L of lymph (including chyle [intestinal lymph]) daily (9).

The lymphatic system plays an important role in fluid balance by returning excess interstitial fluid and proteins to the blood. It is a vital part of the immune system and, along with lymphoid tissues such as the lymph nodes and spleen, clears waste products and cellular debris (including bacteria and proteins). The additional function of the intestinal lymphatic system is the absorption of long-chain lipids from the intestine. For that reason, the concentration of lipids in the intestinal lymph, as well as of proteins (60% of that in the blood), is high. One of the important functions of the hepatic lymphatic system is delivering the proteins that are synthesized by the liver into the bloodstream, and for that reason the concentration of proteins in liver lymph is the highest (80%–90% of that in the blood). The concentration of proteins in the peripheral lymph is low (17%–30% of that in the blood) (10,11). Understanding the biochemical differences of the different types of lymph is crucial in diagnosis of the origin of lymphatic leaks.

Evolution of Imaging of the Lymphatic System

The lymphatic system has traditionally been imaged with direct radiographic lymphangiography through cannulation of peripheral lymphatic ducts on the dorsa of the feet and hands and injection of ethiodized oil–based contrast material. However, cannulation of these small peripheral lymphatic ducts is technically challenging and time consuming. Other methods used to image the peripheral lymphatic system have included interstitial injection of imaging agents that are rapidly absorbed into terminal lymphatic ducts, as has been used in extremity lymphoscintigraphy and extremity lymphangiography (such as when performed at fluoroscopy or MR imaging) (12). Lymphoscintigraphy has been an important technique for evaluation of the lymphatic system, performed by injection of radioactive tracers intracutaneously or subcutaneously in the feet and hands. It provides dynamic information but lacks spatial resolution and anatomic details. MR lymphangiography provides excellent imaging of the lower extremity lymphatic ducts. However, it has never been reported in children. These methods are technically challenging and time consuming (especially in small children) and require longer anesthesia time. More importantly, even though these methods are adequate for visualizing peripheral lymphatic ducts, they are not optimal for visualization of the CCLs, which include the retroperitoneal lymphatic channels, cisterna chyli, and thoracic duct, because of dilution of contrast material by intestinal and hepatic nonopacified lymphatic flow. For improved and selective visualization of the CCLs, injection of contrast material in the inguinal lymph nodes has been attempted for many decades (13). Recently, ultrasonography (US)-guided intranodal injection of oil-based contrast material (similar to US-guided intranodal gadolinium injection,

explained later) with imaging of CCLs at fluoroscopy has been refined for use in children and successfully used for subsequent lymphatic intervention (14,15). This technique provides excellent spatial resolution. Limitations of this technique include exposure to ionizing radiation, longer examination time, limited dynamic information, and limited information about the relationship of lymphatic ducts with surrounding structures (5). Moreover, oil-based contrast material must be used with caution in children with right-to-left shunts from congenital heart disease or from large pulmonary arteriovenous malformations because of the risk for systemic embolism. Cerebral ethiodized-oil embolism after lymphatic embolization has been reported in a child with congenital heart disease and plastic bronchitis, due to direct connection between the lymphatics and the pulmonary venous branch (16).

Lymphatic structures can be visualized in children and adults at T2-weighted MR imaging. Laor et al (12) used T2-weighted imaging to visualize peripheral and central lymphatic ducts in 29 children with various conditions, including Klippel-Trénaunay-Weber syndrome, kaposiform hemangioendothelioma, and Gorham disease, presumably because of extensive and marked lymphatic abnormalities in these conditions. The advantage of using T2-weighted imaging is its ability to demonstrate pathologic lymphatic structures (eg, lymphatic masses, lymphangiectasias, and dilatation of the cisterna chyli and/or thoracic duct) and the presence and distribution of the lymphatic fluid in body cavities. Dori et al (17) demonstrated the feasibility of T2-weighted MR imaging for identification of lymphatic abnormalities in 38 children after single-ventricle palliative surgery, which can be associated with lymphatic abnormalities. However, T2-weighted MR lymphangiography has several limitations. It is a static imaging modality that lacks dynamic information and therefore fails to demonstrate lymphatic reflux or leakage. It may be difficult to visualize smaller lymphatic ducts because of insufficient signal from the small amount of fluid within them. It can also be difficult to differentiate lymphatic ducts from other overlapping fluid-containing structures and veins. Visualization of lymphatic channels may also be limited at T2-weighted imaging owing to artifacts from breathing, peristalsis, and cardiac movement.

To overcome these limitations, Dori et al (3) developed DCE MR lymphangiography by injecting commercially available gadolinium-based contrast material (GBCM) into groin lymph nodes in a porcine model and subsequently used it for planning selective lymphatic embolization in children with plastic bronchitis, which is a rare condition caused by lymphatic perfusion of the lung parenchyma and characterized by expectoration of branching bronchial casts (4,18). This was followed by a detailed description by Krishnamurthy et al (5) of the technique of DCE MR lymphangiography in children and its utilization in six children with various lymphatic conditions. It is potentially more sensitive than fluoroscopic lymphangiography in detecting the leakages in chylous ascites, owing to GBCMs being less viscous than oil-based contrast agents. However, DCE MR lymphangiography has its own limitations and cannot create visualizations of the lymphatic structures outside of the pathway of the contrast material that has been injected into groin lymph nodes. Sometimes the contrast material does not propagate into the thoracic duct because of distal obstruction or leak. In these cases, T2-weighted sequences help with identification of these lymphatic masses and the thoracic duct.

For these reasons, a combination of T2-weighted sequences and DCE MR lymphangiography is a better choice for assessment of CCLs. Our MR lymphangiography protocol includes both T2-weighted and DCE lymphangiography, as described later.

Technique of Dynamic Intranodal MR Lymphangiography

The pediatric patient is placed supine on a detachable MR imaging table, outside the scanning room. The posterior elements of the torso coil are underneath the patient. The anterior elements of the coil are placed when the child is moved into the scanner after lymph node cannulation. The examination is performed under general or local anesthesia, depending on the age of the child.

Groin Lymph Node Cannulation

Performing mapping US is recommended to look for the availability of suitably sized lymph nodes in both inguinal regions before scheduling the patient for MR lymphangiography, particularly in infants.

Both inguinal regions are prepared and draped under sterile conditions. A 22- to 25-gauge needle is placed in the medulla or central part of an inguinal lymph node on each side under US guidance. Angiocatheters can be used but tend to become displaced more easily. A low-volume gentle injection of saline is used to ensure that the needle is appropriately located within the medulla and that there is no extravasation. The needle is connected to 21-inch-long tubing with a three-way stopcock on each end and taped in place (Fig 2). The needle position is again confirmed at saline injection under US visualization. The size of the node increases with the injection (Fig 3). If the needle is not well positioned or extravasation of normal saline is noted, then the needle is repositioned or

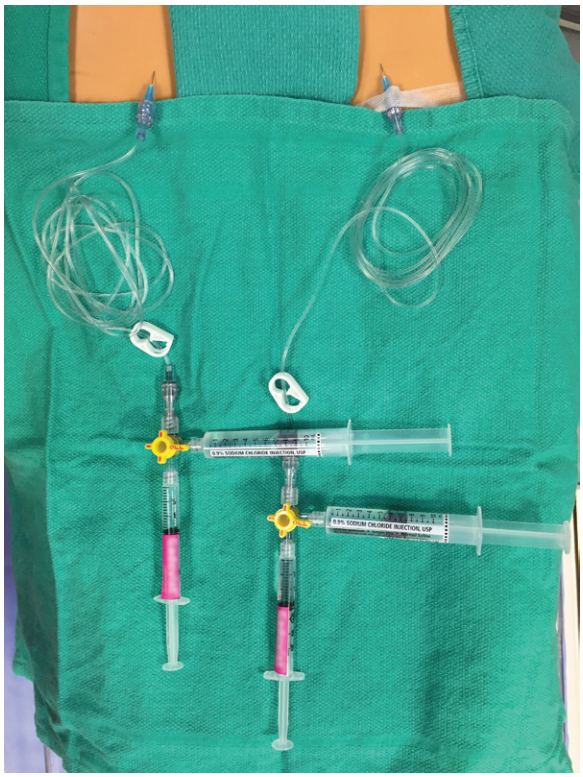

Figure 2. Photograph simulates setup of bilateral groin needles in a phantom. Each needle is connected to 21-inch tubing with a three-way stopcock on the end, which in turn is connected to two syringes, one filled with GBCM and one with saline flush.

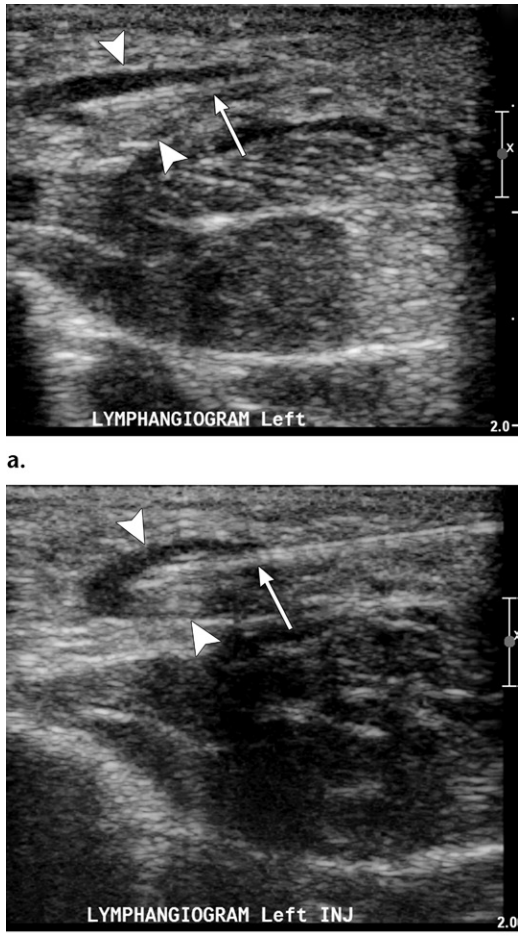

Figure 3. Groin lymph node cannulation for MR lymphangiography in an 8-week-old infant. Longitudinal US images of the left groin before **(a)** and after **(b)** saline injection show a lymph node (arrowheads) with a cannula (arrow) within the central echogenic medulla. The lymph node size increases with injection of saline **(b)**.

another lymph node is accessed. Syringes with contrast material (dilute gadolinium solution) and saline flush are connected to the three-way stopcock (Fig 2). The child is then transferred to the MR imaging machine.

Alternatively, the procedure can be performed in a hybrid imaging suite that combines an MR imaging machine and angiography equipment. The two systems are connected by a shared table that can travel between these two units. The advantage of this system is the ability to place the needles into the lymph nodes using US guidance outside the MR imaging equipment, followed by confirmation of the position of the needle using contrast material injection in the catheterization laboratory. The shared table allows minimal movement of the patient during transport, thus minimizing the chances of needle dislodgement (18).

Contrast Material

Any routinely used macrocyclic GBCM can be used for DCE MR lymphangiography. The dose used is the same standard dose of 0.1 mmol/kg of body weight used for routine intravenous injection. A double dose of 0.2 mmol/kg is used occasionally in larger patients. The guidelines and precautions used for intravenous injection of GBCM, including assessment of renal function, should be followed for DCE MR lymphangiography. The total amount of GBCM can be diluted with normal saline 1:1 for older children and 1:2 for younger children to reduce T2 effects of concentrated gadolinium causing darkening (5). Higher dilution in younger children increases the volume available for injection. Some centers do not dilute the contrast material. The total volume is divided, and half of the amount is injected on each side. The entire tubing is primed with contrast material–containing solution. A syringe with normal saline is also attached to a three-way stopcock on each side to flush the system and push the contrast material remaining in the tube.

MR Imaging Examination

Hardware and Coverage.—Better signal and smaller voxels can be achieved on 3-T scanners than on 1.5-T scanners (19). This can potentially

result in better visualization of thin lymphatic ducts. However, MR lymphangiography can be performed on 1.5-T scanners, and in fact, all of the initially reported studies have been performed on 1.5-T scanners (4,5,18). The typical coverage for DCE MR lymphangiography extends from the lesser trochanter to midneck. Coil choice may change with the size of the patient. Typically, most smaller children under anesthesia can be imaged with torso coils. A plastic tray can be placed over the abdomen and pelvis to lift the weight of the anterior coil off the patient, to protect the sterile field and minimize dislodgement of the tubing and cannulae (5).

Sequences.—The MR pulse sequences acquired in a particular sequence are listed in the Table. The two main components are T2-weighted imaging and postcontrast dynamic T1-weighted imaging. The regular T2-weighted imaging (TE, 80–100 msec) in the axial or coronal plane provides an overall evaluation of the anatomy and any gross abnormality. This is followed by a heavily T2-weighted 3D sequence (eg, MR cholangiopancreatography) for visualization of the lymphatic ducts. Single-shot T2-weighted thin-section images with a moderate TE of 160 msec are useful for visualization of thin ducts that may be poorly visualized at imaging with a high TE of 700–800 msec owing to the small amount of fluid within them. T2-weighted images help to localize areas of lymphedema. They also provide anatomic information about the cisterna chyli and thoracic duct. There are no data on the frequency of visualization of the cisterna chyli and thoracic duct on heavily T2-weighted images. However, on routine T2-weighted images, these structures are visualized in only approximately 15% of patients (8).

Dynamic postcontrast imaging of the initial movement of contrast material after injection (first passage of contrast material) through the ducts is performed by using T1-weighted 3D gradient sequences such as THRIVE/VIBE/LAVA in the coronal plane that can be acquired in 15–30 seconds. First, a mask image is acquired that is used for subtraction. Then, from the start of intranodal contrast material injection, images are acquired every minute until the contrast material reaches the venous angle where the thoracic duct drains. More frequent imaging (every 30 seconds) can be performed if there is chylolymphatic reflux, defined as passage of contrast agent from the CCLs into lymphatic ducts away from the expected direction of flow. Images in the axial plane can be acquired as required to assess the ducts. Washout of contrast agent from normal lymphatic ducts typically occurs in 15–30 minutes (5). If washout needs to be documented, a delayed run can be performed

MR Lymphangiography Protocol

Sequence No.	Sequence	Plane	TR/TE (msec/msec)	Flip Angle (degrees)	Matrix	ST (mm)	ETL	NSA	Pixel Bandwidth (Hz)	Approximate Time
1	FSE T2W	Axial	2174/80	90	316 × 211	4	24	2	280	5 min
2	Fat-saturated single-shot T2W	Coronal	2248/160	90	264 × 230	3	96	1	399	3 min
3	Fat-saturated single-shot T2W	Axial	1376/160	90	268 × 237	3	98	1	404	4 min
4	3D FSE T2W	Coronal	3168/740	180	288 × 256	2	129	1	167	4 min
5	3D GRE T1W (VIBE/THRIVE/LAVA)	Coronal	3.5/1.7	10	308 × 362	2.6	1	1	574	20–30 sec
GBCM 0.1 mmol/kg, 1:1 or 1:2 dilution; half dose in lymph node on each side of the groin, slowly hand injected (approximately 0.5–1 mL/min)										
6	3D GRE T1W (VIBE/THRIVE/LAVA) every minute until contrast agent seen at the venous angle	Coronal	3.5/1.7	10	308 × 362	2.6	1	1	574	20–30 sec
7	3D GRE T1W (VIBE/THRIVE/LAVA) as required	Axial	3.1/1.5	10	180 × 180	3	1	1	720	20–30 sec

Note.—ETL = echo train length, FSE = fast spin-echo, GRE = gradient echo, LAVA = liver acquisition with volume acquisition, NSA = number of signal averages, ST = section thickness, TE = echo time, 3D = three-dimensional, THRIVE = T1W high-resolution isotropic volume examination, T1W = T1 weighted, TR = repetition time, T2W = T2 weighted, VIBE = volumetric interpolated breath-hold examination.

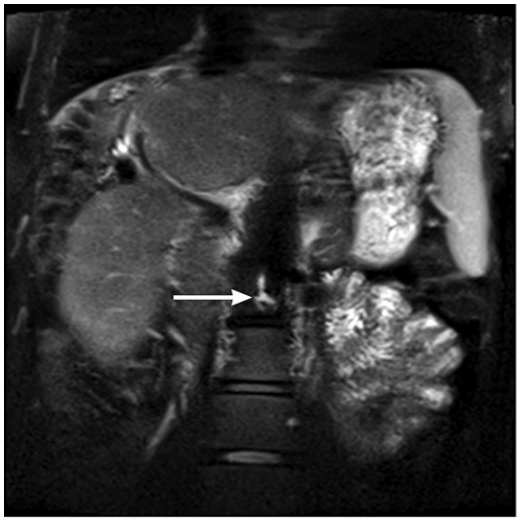

a.

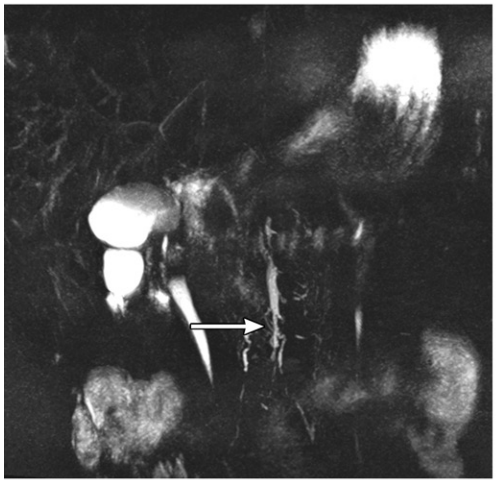

b.

c.

Figure 4. Variable morphology of the cisterna chyli. **(a)** Coronal T2-weighted image of the abdomen in a 6-year-old girl with a history of hepatoblastoma shows a triangular cisterna chyli (arrow). **(b)** Coronal T2-weighted MR cholangiopancreatographic image in a 17-year-old adolescent boy with primary sclerosing cholangitis demonstrates a long tubular cisterna chyli (arrow) joined by lumbar trunks. **(c)** Coronal T2-weighted MR cholangiopancreatographic image in a different 17-year-old adolescent boy with primary sclerosing cholangitis demonstrates a thin tubular cisterna chyli (arrow) with a much thicker and tortuous lymphatic duct (arrowheads).

at 30 minutes from the start of intranodal injection. The dynamic coronal images are reformatted using maximum intensity projection (MIP).

After MR Imaging Examination

A follow-up clinical examination is performed after 4 hours to look for any local (eg, skin damage to adjacent to lymph nodes, skin discharge, hematoma) or systemic (eg, those related to anesthesia) complications.

Analysis of Images

What Is Normal?

The anatomic variability of the lymphatic system is significant, primarily due to complex embryologic development (7). In addition, the first applications of MR lymphangiography techniques have been in patients with lymphatic disorders. For that reason, knowledge of normal lymphatic anatomy is limited. The cisterna chyli can be highly variable in its shape and size and can appear as a single straight tube, straight thick tube, sausage-shaped tube, tortuous tube, or focal plexus (8) (Fig 4). In some cases, there may not be an identifiable cisterna chyli (Fig 5). The thoracic duct can have a variable diameter along its course. It may normally show significant tortuosity. The lymphatic ducts are also slightly more tortuous than the venous system and can have an interrupted appearance at intervals, caused by constrictions at the valve locations (6). This knotted or beaded appearance of the lymphatic ducts can help to differentiate them from other channels such as small veins (Fig 6).

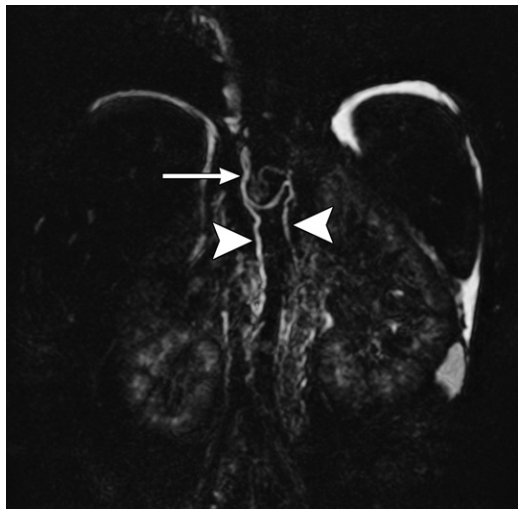

Figure 5. Variable morphology of the thoracic duct. Coronal T2-weighted MR cholangiopancreatographic image in a 4-year-old girl with previous pancreatitis demonstrates two large trunks (arrowheads) forming a thoracic duct (arrow), which is located more on the right side of the spine than usual. There is no clear cisterna chyli in this child.

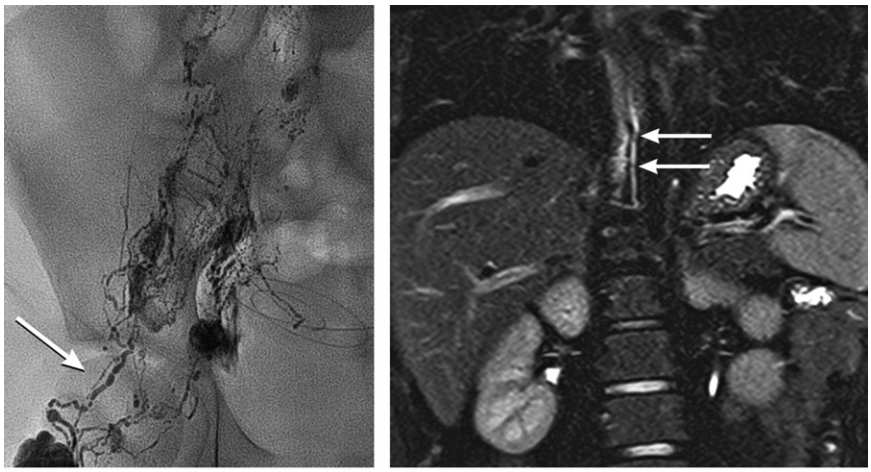

a. **b.**

Figure 6. Knotted appearance of lymphatic channels. **(a)** Image from conventional intranodal lymphangiography with ethiodized oil in a 12-year-old girl with a renal transplant demonstrates a knotted appearance (arrow) of lymphatic channels relating to valves. **(b)** Coronal T2-weighted MR image in a 17-year-old adolescent boy with nonspecific abdominal pain demonstrates a similarly knotted appearance (arrows) of a normal thoracic duct.

First passage of contrast material.—After the start of intranodal injection (Fig 7), contrast material typically appears in the retroperitoneal lymphatics at the aortic bifurcation and along the iliac ducts within 2 minutes. A normal cisterna chyli is opacified in 3–6 minutes. Thereafter, the passage of contrast material superiorly from the cisterna chyli is rapid and reaches the venous angle through the thoracic duct approximately in the next 2–3 minutes (5). Contrast material is typically washed out from the normal CCL in 15–20 minutes and is accompanied by renal enhancement and excretion (5).

What Is Abnormal?

Lymphangiectasia is dilatation of the lymphatic vessels. The presence of several lymphatic channels in the same region with flow in a similar direction is termed *collateralization* (5). Collateralization indicates abnormal drainage of the lymphatic system. Thoracic duct dilatation, lymphangiectasia, and collateralization can be seen with proximal obstruction or congestion of the lymphatic system due to elevated central venous pressure (Fig 8). Lymphangiectasia seen at DCE MR lymphangiography has been correlated with decreased lymphatic drainage at lymphoscintigraphy, indicating that it is most probably due to obstruction to the flow (20). Normally, lymph drains from the peripheral to the central conducting ducts and ultimately to the venous system via the thoracic duct. Passage of contrast agent from the CCLs into the lymphatic ducts away from the expected direction of flow is termed *chylolymphatic reflux* (retrograde lymphatic flow). Additional abnormalities that can

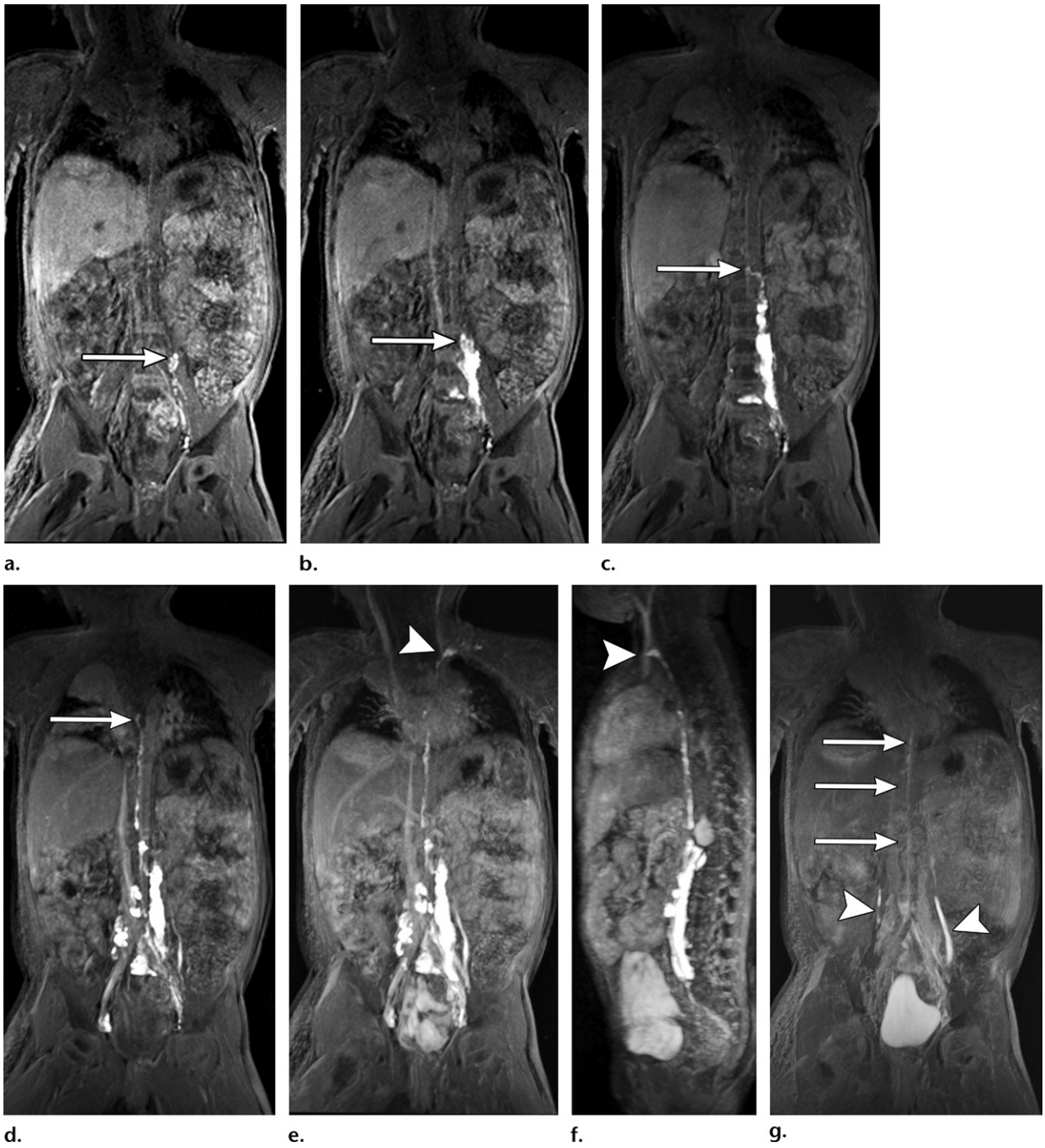

Figure 7. First passage of contrast material after groin intranodal injection up to the venous angle in a 2-year-old child with protein-losing enteropathy and areas of lymphedema in the extremities. CCLs were interpreted to be normal in this child. **(a–e)** Coronal 3D T1-weighted images with thin MIP reconstruction at 2 **(a)**, 4 **(b)**, 6 **(c)**, 8 **(d)**, and 11 **(e)** minutes after injection of contrast material demonstrate progressive passage of the contrast material (arrow) up to the venous angle (arrowhead in **e**). **(f)** Sagittal oblique MIP reconstruction from the 14-minute acquisition demonstrates the entire CCLs and the venous angle (arrowhead). **(g)** Coronal 3D T1-weighted image with thin MIP reconstruction at 30 minutes after contrast agent injection demonstrates almost complete washout of contrast agent from the CCLs (arrows) with excretion in the ureters (arrowheads) and urinary bladder.

be seen include obstruction of a segment and leakage from the lymphatic channels and thoracic duct. Pleural and pericardial leakage can be seen as an area of progressive accumulation of contrast material followed by slow dispersion (5). Lymphedema is seen as ill-defined areas of heterogeneously increased signal abnormality on T2-weighted images in the soft tissues, predominantly in subcutaneous tissues that are also hypertrophied. It represents lymphatic stagnation due to abnormal lymphatic drainage of the affected area from various causes.

Current and Potential Applications

DCE MR lymphangiography is a recently developed technique, and its clinical applications are

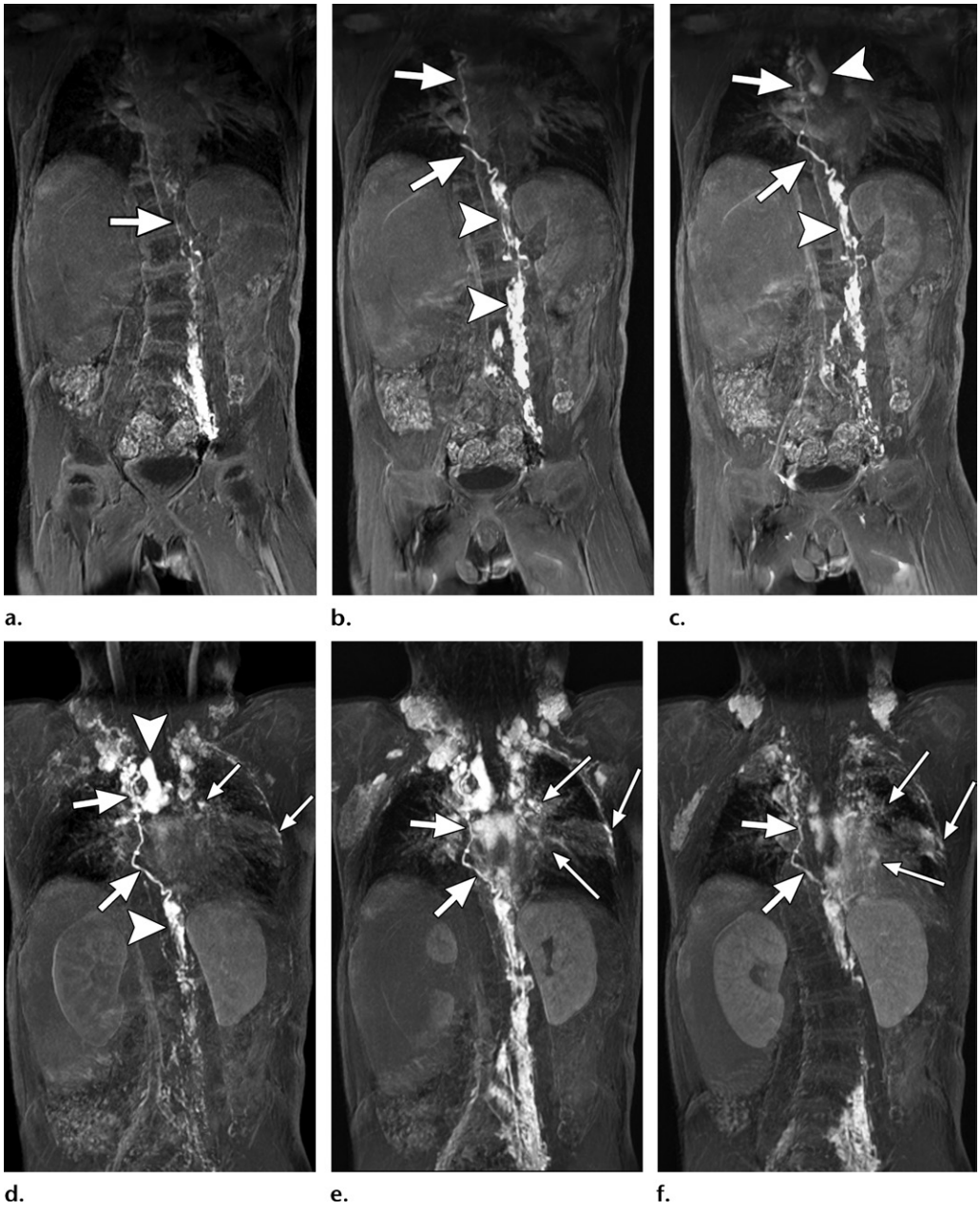

Figure 8. MR lymphangiography in an 8-year-old child with a history of Fontan surgery and plastic bronchitis. Coronal 3D T1-weighted images with thin MIP reconstruction at 2 **(a)**, 4 **(b)**, 6 **(c)**, 8 **(d)**, 10 **(e)**, and 20 **(f)** minutes after injection of contrast material demonstrate an abnormal lymphatic duct extending from the retroperitoneum to the right side of the superior mediastinum (thick arrows), lymphangiectasia in the retroperitoneum (arrowheads) and mediastinum (arrowheads), and extensive and progressive chylolymphatic reflux into cervical and axillary lymph nodes. There is no clear visualization of a typical thoracic duct. The delayed images **(e, f)** also demonstrate chylolymphatic reflux into the left lung, pleural region, and right lung apex (thin arrows) suggesting pulmonary lymphatic perfusion syndrome (PLPS) as the cause of the plastic bronchitis.

still emerging. One of the common indications for DCE MR lymphangiography is evaluation of PLPS, which forms the basis for conditions such as plastic bronchitis, neonatal lymphatic flow disorders, lymphatic malformations, idiopathic chylothorax, and chylothorax in children after cardiac surgery. Other conditions for which it can be used include chylothorax and chylous ascites from other causes, as discussed later.

Pulmonary Lymphatic Perfusion Syndrome

Normally, the lymphatic flow from the lung parenchyma is to the thoracic duct. PLPS is a condition in which there is a congenital abnormal pulmonary lymphatic flow away from the thoracic duct toward the lung parenchyma and mediastinum and through the aberrant lymphatic vessels. PLPS can manifest at any age, from newborns as a neonatal chylothorax to older children or adults as an idio-

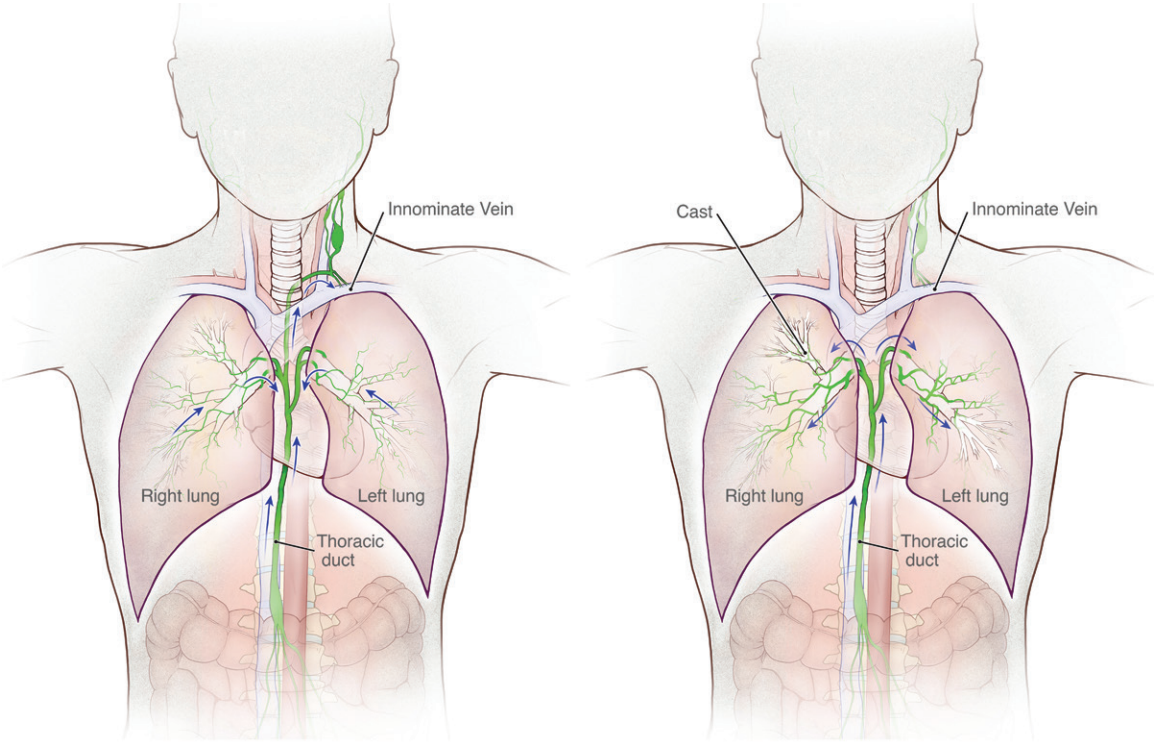

a. b.

Figure 9. **(a)** Schematic representation of normal flow in the thoracic duct and pulmonary lymphatic vessels. **(b)** Schematic representation of lymphatic flow from the thoracic duct toward the pulmonary parenchyma in patients with PLPS. (Reprinted, with permission, from The Children's Hospital of Philadelphia, Philadelphia, Pa.)

pathic chylothorax or lymphatic or plastic bronchitis (21). It is hypothesized that aberrant lymphatic collaterals develop because of in utero occlusion or stenosis of the downstream segment of the thoracic duct (22). They are not often clinically significant. However, they may become symptomatic if the collaterals abut the serous and mucosal surfaces, such as the pleura, pericardia, and bronchi, leading to leakage from them under provocation by silent trauma, severe respiratory infection, or increased central venous pressure in patients with Fontan circulation. Typical DCE MR lymphangiography findings of PLPS include retrograde flow of the contrast material toward the lung parenchyma and occlusion or stenosis of the superior segment of the thoracic duct (Fig 9) (22). DCE MR lymphangiography helps in planning the intervention by showing anatomy such as single or double thoracic duct, presence of communication between different branches, and absence or narrowing of the distal part of the thoracic duct.

Plastic Bronchitis.—Plastic bronchitis is a rare condition characterized by expectoration of branching bronchial casts (18). Airway obstruction caused by casts can lead to significant asphyxia and can be fatal. The branching cast is formed by exudation of proteinaceous material and cells in the airways. Plastic bronchitis can occur in patients after single-ventricle palliation, cystic fibrosis, sickle cell anemia, asthma, and lymphangiomatosis (23,24). In patients with total cavopulmonary connection, the prevalence of plastic bronchitis is approximately 4% (25). PLPS serves as an anatomic substrate for the condition. Elevated central venous pressure in these patients results in increased production of lymph as well as an increase in impedance to lymphatic drainage (4). This results in congestion in the central lymphatic system and in PLPS can result in overflow of lymph into the lung parenchyma. This abnormal lymphatic flow into the lungs causes protein leakage into the airways and cast formation (4,18). Dilatation of subpleural and interlobular lymphatics has been shown in patients with plastic bronchitis and intestinal lymphangiectasia in patients with protein-losing enteropathy demonstrated at pathologic analysis (26). Abnormal tracer uptake in lungs with plastic bronchitis has been noted at lymphoscintigraphy (18). Findings at DCE MR lymphangiography in these patients include abnormal lymphatic flow from the thoracic duct toward the pulmonary parenchyma (4,17,18) (Fig 10). Medical treatments for plastic bronchitis such as phosphodiesterase type 5 inhibitors, steroids, and mucolytics only improve symptoms and do not treat the underlying condition. Cardiac

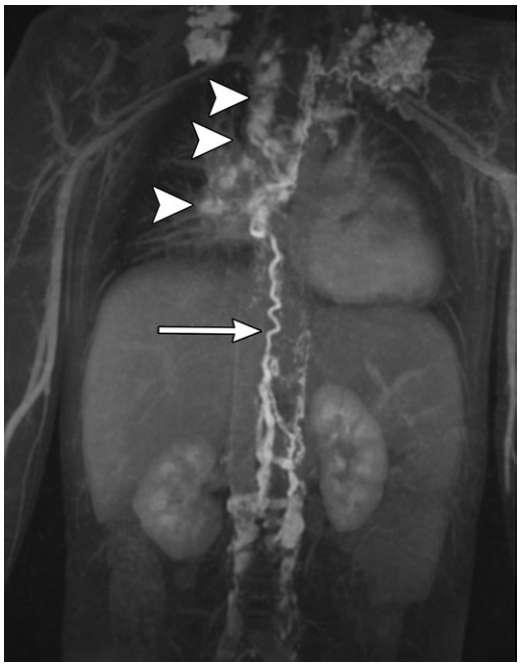

Figure 10. Plastic bronchitis in a 6-year-old boy after Fontan surgery. DCE MR lymphangiogram demonstrates retrograde pulmonary lymphatic enhancement (arrowheads) that originates in the thoracic duct (arrow). This finding is consistent with PLPS.

Figure 11. Neonatal chylothorax in a 6-week-old male infant. DCE MR lymphangiogram demonstrates pulmonary lymphatic enhancement (arrowheads) consistent with PLPS.

transplantation can lead to resolution of plastic bronchitis, presumably due to normalization of central venous pressure and return of normal pulsatile pulmonary flow (as opposed to the passive flow of Fontan circulation). More recently, selective embolization of lymphatic channels in the lungs and thoracic duct stent placement have been successfully used to treat the disease in children and adults, with a close to 90% success rate (4,18,27). DCE MR lymphangiography is essential in planning embolization treatment for patients with plastic bronchitis. One of its most important uses is the identification of all lymphatic pathways from the abdomen toward the chest. These communications can consist of a single thoracic duct or two thoracic ducts or can be through the retroperitoneal/mediastinal pathways.

Neonatal Lymphatic Flow Disorders.—Neonatal lymphatic flow disorders can be detected in utero as hydrops fetalis, chylous ascites, or chylothorax. DCE MR lymphangiography can be used to differentiate among three different types: isolated chylothorax, congenital lymphatic dysplasia, and congenital chylous ascites.

In most cases, isolated neonatal chylothorax is discovered at prenatal US (28). A thoracoamniotic shunt is then placed to prevent underdevelopment of the lung (29). In patients with isolated neonatal chylothorax, DCE MR lymphangiography demonstrates lymphatic flow from the thoracic duct toward the pulmonary parenchyma and absence of the upper part of the thoracic duct (indicative of PLPS) (Fig 11). Pulmonary lymphangiectasia can manifest as a nutmeg appearance of the lungs at fetal MR imaging (30). Embolization of this pulmonary lymphatic flow with ethiodized oil can result in complete resolution of the chylothorax (31).

Congenital lymphatic dysplasia manifests as any combination of chylothorax, chylous ascites, pericardial effusion, and/or soft-tissue edema and is often diagnosed as a nonimmune hydrops (32,33). At DCE MR lymphangiography, the hallmarks of this condition are absent or diminished central lymphatic flow and the presence of dermal lymphatic flow. There are limited treatment options for this condition. If the thoracic duct is found to be occluded at the level of the neck, a microsurgical thoracic duct–to-vein connection can be attempted. Percutaneous embolization is contraindicated in these cases.

Isolated chylous ascites in neonates can also be detected at prenatal US. After birth, findings at T2-weighted MR lymphangiography include high-signal-intensity lymphatic masses that enhance at DCE MR lymphangiography. In some cases, frank extravasation of the contrast material into the abdominal cavity can be detected (Fig 12).

Lymphatic Malformations.—The term *lymphatic malformations* refers to a group of poorly defined

Figure 12. Congenital chylous ascites from chylous leak in an 8-week-old infant (same patient as in Fig 3). **(a–c)** Coronal 3D T1-weighted images at 1 **(a)**, 3 **(b)**, and 12 **(c)** minutes after injection of contrast material demonstrate chyle from a retroperitoneal lymphatic channel (arrow in **a** and **b**) with progressive opacification of the left side of the abdomen. **(d)** Subsequent conventional intranodal lymphangiogram obtained with intranodal injection of ethiodized oil demonstrates the leak (arrow). **(e)** Follow-up conventional intranodal lymphangiogram with intranodal injection of ethiodized oil obtained 5 months later does not show any leak. It demonstrates the thoracic duct (arrowheads), which was not visualized previously, and new lymphatic channels (arrow) in the retroperitoneum. Ethiodized oil injection during the conventional lymphangiography also served as therapeutic reduction of the leak. After needle disruption of the leaking lymphatic vessel, the child has had stable mild ascites requiring no further drainage.

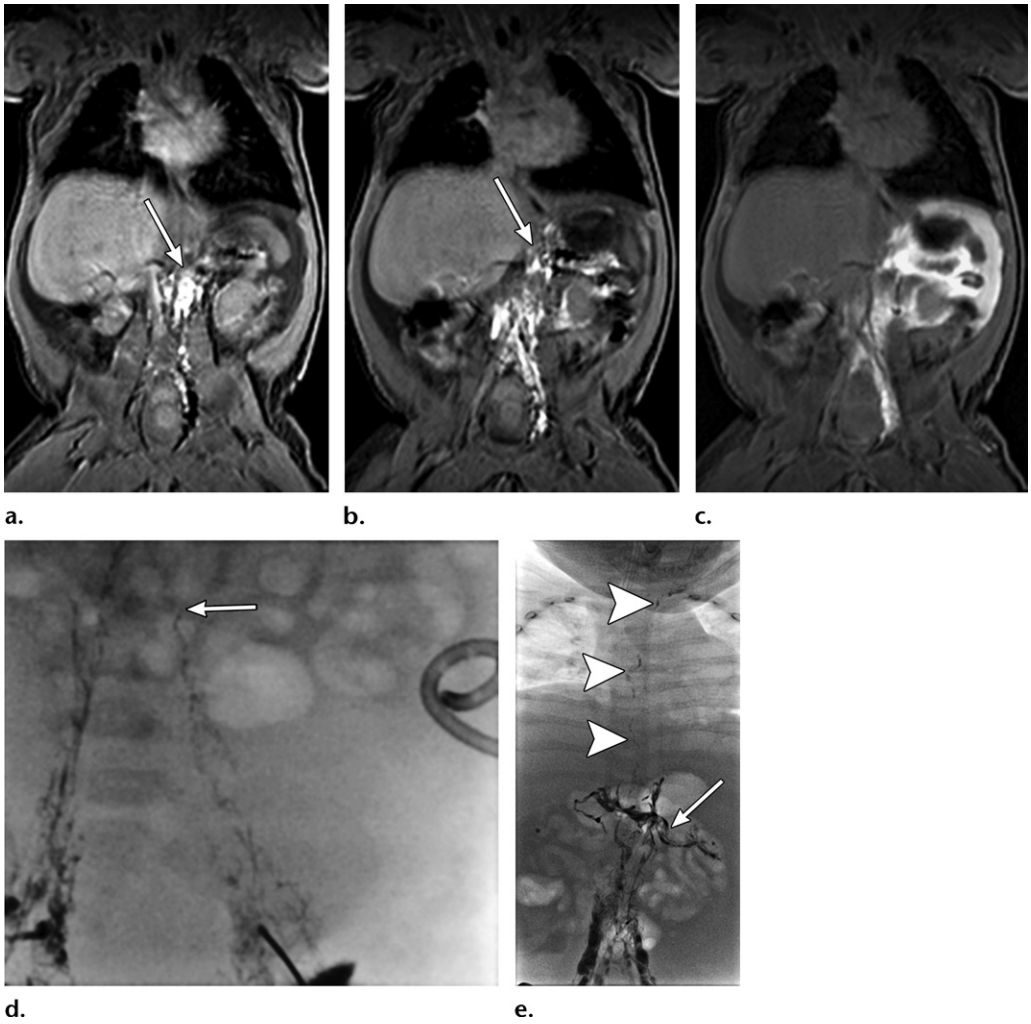

developmental lymphatic anomalies that include conductive lymphatic disorders, generalized lymphatic anomaly, Gorham disease, and kaposiform lymphangiomatosis (a proliferative disorder) (34). The main cause of morbidity and mortality in these patients is deterioration of pulmonary function due to interstitial lung disease and chylothorax.

MR lymphangiography in these conditions often shows pleural effusions, significant dilatation of the thoracic duct at T2-weighted imaging, and PLPS. The PLPS in this instance can originate from the thoracic duct or from the retroperitoneal lymphatic networks (Fig 13). This abnormal pulmonary flow can result in pleural effusion that results in either passive atelectasis of the lung or interstitial lung disease. The cessation of this cranial lymphatic flow from the abdomen toward the lungs can potentially prevent damage of lung tissue and prolong the patient's life.

Idiopathic Chylothorax.—*Idiopathic chylothorax* is defined as isolated chylothorax without identifiable causes (eg, trauma, systemic disease, or malignancy). Over the years, one of the main challenges in treatment of idiopathic chylothorax has been identification and characterization of the lymphatic anatomy. In some cases, even intranodal fluoroscopic lymphangiography could not provide adequate imaging of the central and pulmonary lymphatic systems. DCE MR lymphangiography can provide excellent imaging of lymphatic abnormalities in this patient population. As with

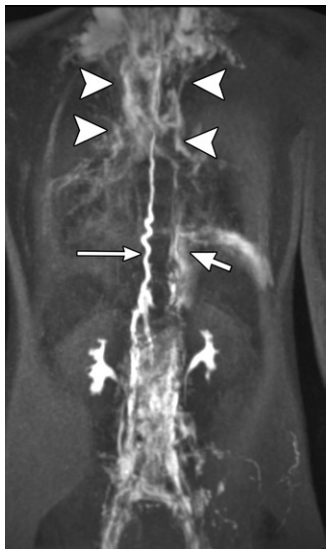

Figure 13. Kaposiform lymphangiomatosis in a 2-year-old girl. DCE MR lymphangiogram demonstrates abnormal pulmonary lymphatic enhancement from the thoracic duct (long arrow) toward the pulmonary parenchyma (arrowheads). There is lymphatic enhancement that originates in the left retroperitoneum and extends into the mediastinum (short arrow).

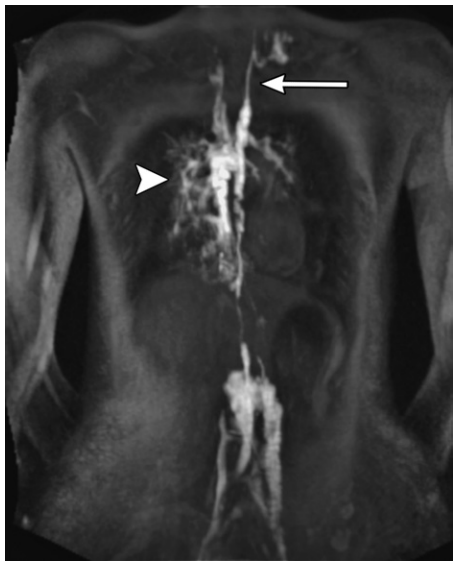

Figure 14. Idiopathic chylothorax in a 6-year-old child. DCE MR lymphangiogram demonstrates narrowing (arrow) of the upper part of the thoracic duct and abnormal pulmonary lymphatic enhancement (arrowhead) consistent with PLPS. (Reprinted, with permission, from reference 22.)

patients with PLPS, in most patients with idiopathic chylothorax there is abnormal pulmonary lymphatic flow from the thoracic duct toward the lung parenchyma (Fig 14). In addition, dilatation of the thoracic duct is often observed in these patients.

Chylothorax in Pediatric Patients After Cardiac Surgery.—Surgery for congenital cardiac disease is a common and important cause of chylothorax in children, with an incidence of 2.8%–3.9% (35,36). It is associated with increased mortality, cost, and length of hospital stay (35). Until recently, it had been assumed that the cause of chylothorax is physical trauma to the thoracic duct or its branches. However, a recent review by Savla et al (37) that used DCE MR lymphangiography and intranodal lymphangiography to image 25 patients showed that trauma to the thoracic lymphatic duct occurred in only two (8%) of the patients. A majority of the patients, 14 (56%), had PLPS. Nine patients (36%) had central lymphatic flow disorder, which is characterized by abnormal central lymphatic flow, effusion in more than one compartment, and dermal backflow. Imaging findings of PLPS in these patients are very similar to the imaging findings in patients with plastic bronchitis. Few patients in this series presented with a combination of plastic bronchitis and chylothorax.

Other Causes of Chylothorax and Chylous Ascites

Chylous pleural effusion and ascites can result from inadequate chylous transport through or leakage from the CCLs, due to several causes. Idiopathic chylopericardium can result from the same causes, but it is rarer. Chylothorax and chylous ascites can be congenital and may result from aplasia, hypoplasia, obstruction, valvular incompetence, or leakage from the thoracic duct. Congenital chylothorax can be associated with several syndromes, including Noonan, Down, and Turner syndromes (9). The reason for this association is not known. Other causes include trauma (including traumatic delivery, thoracic surgery, or abdominal surgery), lymphatic malformations, malignant tumors, and infections (eg, tuberculosis or fungal) (9,38). Chylothorax can result from thrombosis of the superior vena cava or subclavian veins, likely due to resistance to the flow of lymph from the lymphatic duct into the veins.

Chylothorax can lead to malnutrition and immunodeficiency. Chylothorax and chylous ascites have been treated with drainage, dietary modifications, and medical therapy with secretion inhibitors such as octreotide or somatostatin. Refractory cases are treated with pleurodesis, pleuroperitoneal shunts, surgical ligation, or embolization of the thoracic duct (9,38).

The leakage of chyle in patients with chylous ascites can occur anywhere on the pathway that includes the intestinal lymphatic ducts, cisterna chyli, and lower part of the thoracic duct. Unfortunately, leakage from the intestinal lymphatic channels before they join the intestinal trunks at the cisterna chyli will not be detected at DCE MR lymphangiography, as they are outside the opacified central lymphatics. For that reason, its results are negative in most cases of chylous ascites.

However, DCE MR lymphangiography can still potentially be a more sensitive method to

detect the leakages in chylous ascites because of the physical properties of GBCMs that make them less viscous than oil-based contrast materials. For that reason, we use DCE MR lymphangiography in all patients with chylous ascites. The typical imaging finding in a patient with chylous ascites is extravasation of contrast material into the peritoneal cavity (Fig 12). In some cases of chylothorax and chylous ascites, MR lymphangiography will help to show preserved integrity of the CCLs. In addition to its diagnostic utility, MR lymphangiographic images can be fused with those from C-arm imaging to aid in localization of the cisterna chyli during percutaneous lymphatic intervention.

Other Potential Applications

As with any new imaging modality, the list of applications of DCE MR lymphangiography is likely to grow substantially as the understanding of the lymphatic basis for many diseases increases. Some diseases are known to have a lymphatic component in their pathophysiology. However, it is possible that some of the unexplained symptoms in patients with conditions that are not thought to be of lymphatic origin can be explained and imaged with DCE MR lymphangiography as well. An example of this is congenital intestinal lymphangiectasia with associated protein-losing enteropathy. Protein-losing enteropathy is a significant complication of Fontan circulation, likely originating from liver lymphatics. Even though DCE MR lymphangiography cannot reliably image normal intraperitoneal and intestinal lymphatics, it could demonstrate findings of lymphatic congestion in CCLs in patients with Fontan circulation and normal CCLs in congenital intestinal lymphangiectasia (Fig 5). DCE MR lymphangiography can be used to assess any ductal abnormality in communication with lymphatic malformations or large lymphatic cysts (5). It is possible that PLPS explains some of the symptoms in patients with unexplained pulmonary symptoms, such as chronic cough and interstitial lung disease. The potential applications of DCE MR lymphangiography in patients with heart failure are waiting to be discovered. DCE MR lymphangiography could also be useful in extremity lymphedema and generalized lymphatic dysplasia to assess the status of the CCLs. DCE MR lymphangiography could have oncologic applications to localize sentinel lymph nodes and drainage pathways.

Conclusion

DCE MR lymphangiography for the assessment of CCLs, including the retroperitoneal lymphatics, cisterna chyli, and thoracic duct, is performed by injecting GBCM into the groin nodes. T2-weighted imaging plays a complementary role in assessment of the CCLs. It is quicker than conventional fluoroscopic lymphangiography and lymphoscintigraphy and can be performed in children who have right-to-left shunt. DCE MR lymphangiography provides information about CCL anatomy or abnormalities such as blockages, leaks, and abnormal lymphatic perfusion. The technique has been successfully used for understanding of the lymphatic anatomy and planning of percutaneous embolization in patients with plastic bronchitis, nontraumatic chylothorax, and neonatal lymphatic disorders.

References

1. Itkin M, Krishnamurthy G, Naim MY, Bird GL, Keller MS. Percutaneous thoracic duct embolization as a treatment for intrathoracic chyle leaks in infants. Pediatrics 2011;128(1):e237–e241.
2. Nadolski GJ, Itkin M. Thoracic duct embolization for nontraumatic chylous effusion: experience in 34 patients. Chest 2013;143(1):158–163.
3. Dori Y, Zviman MM, Itkin M. Dynamic contrast-enhanced MR lymphangiography: feasibility study in swine. Radiology 2014;273(2):410–416.
4. Dori Y, Keller MS, Rychik J, Itkin M. Successful treatment of plastic bronchitis by selective lymphatic embolization in a Fontan patient. Pediatrics 2014;134(2):e590–e595.
5. Krishnamurthy R, Hernandez A, Kavuk S, Annam A, Pimpalwar S. Imaging the central conducting lymphatics: initial experience with dynamic MR lymphangiography. Radiology 2015;274(3):871–878.
6. Gray H. The lymphatic system. In: Lewis WH, ed. Anatomy of the human body. 20th ed. New York, NY: Bartleby.com, 2000. http://www.bartleby.com/107/175.html. Accessed February 8, 2017.
7. Hsu MC, Itkin M. Lymphatic anatomy. Tech Vasc Interv Radiol 2016;19(4):247–254.
8. Pinto PS, Sirlin CB, Andrade-Barreto OA, Brown MA, Mindelzun RE, Mattrey RF. Cisterna chyli at routine abdominal MR imaging: a normal anatomic structure in the retrocrural space. RadioGraphics 2004;24(3):809–817.
9. Tutor JD. Chylothorax in infants and children. Pediatrics 2014;133(4):722–733.
10. Szabó G, Pósch E, Magyar Z. Interstitial fluid, lymph and oedema formation. Acta Physiol Acad Sci Hung 1980;56(4):367–378.
11. Witte CL, Witte MH, Dumont AE, Cole WR, Smith JR. Protein content in lymph and edema fluid in congestive heart failure. Circulation 1969;40(5):623–630.
12. Laor T, Hoffer FA, Burrows PE, Kozakewich HP. MR lymphangiography in infants, children, and young adults. AJR Am J Roentgenol 1998;171(4):1111–1117.
13. Hall RC, Krementz ET. Lymphangiography by lymph-node injection. JAMA 1967;202(13):1136–1139.
14. Rajebi MR, Chaudry G, Padua HM, et al. Intranodal lymphangiography: feasibility and preliminary experience in children. J Vasc Interv Radiol 2011;22(9):1300–1305.
15. Nadolski GJ, Itkin M. Feasibility of ultrasound-guided intranodal lymphangiogram for thoracic duct embolization. J Vasc Interv Radiol 2012;23(5):613–616.
16. Kirschen MP, Dori Y, Itkin M, Licht DJ, Ichord R, Vossough A. Cerebral lipiodol embolism after lymphatic embolization for plastic bronchitis. J Pediatr 2016;176:200–203.
17. Dori Y, Keller MS, Fogel MA, et al. MRI of lymphatic abnormalities after functional single-ventricle palliation surgery. AJR Am J Roentgenol 2014;203(2):426–431.
18. Dori Y, Keller MS, Rome JJ, et al. Percutaneous lymphatic embolization of abnormal pulmonary lymphatic flow as treatment of plastic bronchitis in patients with congenital heart disease. Circulation 2016;133(12):1160–1170.

19. Chavhan GB, Babyn PS, Singh M, Vidarsson L, Shroff M. MR imaging at 3.0 T in children: technical differences, safety issues, and initial experience. RadioGraphics 2009;29(5):1451–1466.
20. Notohamiprodjo M, Weiss M, Baumeister RG, et al. MR lymphangiography at 3.0 T: correlation with lymphoscintigraphy. Radiology 2012;264(1):78–87.
21. Itkin M, McCormack FX. Nonmalignant adult thoracic lymphatic disorders. Clin Chest Med 2016;37(3):409–420.
22. Itkin M. Interventional treatment of pulmonary lymphatic anomalies. Tech Vasc Interv Radiol 2016;19(4):299–304.
23. Seear M, Hui H, Magee F, Bohn D, Cutz E. Bronchial casts in children: a proposed classification based on nine cases and a review of the literature. Am J Respir Crit Care Med 1997;155(1):364–370.
24. Madsen P, Shah SA, Rubin BK. Plastic bronchitis: new insights and a classification scheme. Paediatr Respir Rev 2005;6(4):292–300.
25. Schumacher KR, Singh TP, Kuebler J, Aprile K, O'Brien M, Blume ED. Risk factors and outcome of Fontan-associated plastic bronchitis: a case-control study. J Am Heart Assoc 2014;3(2):e000865.
26. Languepin J, Scheinmann P, Mahut B, et al. Bronchial casts in children with cardiopathies: the role of pulmonary lymphatic abnormalities. Pediatr Pulmonol 1999;28(5):329–336.
27. Itkin MG, McCormack FX, Dori Y. Diagnosis and treatment of lymphatic plastic bronchitis in adults using advanced lymphatic imaging and percutaneous embolization. Ann Am Thorac Soc 2016;13(10):1689–1696.
28. Rocha G, Fernandes P, Rocha P, Quintas C, Martins T, Proença E. Pleural effusions in the neonate. Acta Paediatr 2006;95(7):791–798.
29. Wilson RD, Baxter JK, Johnson MP, et al. Thoracoamniotic shunts: fetal treatment of pleural effusions and congenital cystic adenomatoid malformations. Fetal Diagn Ther 2004;19(5):413–420.
30. Victoria T, Andronikou S. The fetal MR appearance of 'nutmeg lung': findings in 8 cases linked to pulmonary lymphangiectasia. Pediatr Radiol 2014;44(10):1237–1242.
31. Gray M, Kovatis KZ, Stuart T, et al. Treatment of congenital pulmonary lymphangiectasia using ethiodized oil lymphangiography. J Perinatol 2014;34(9):720–722.
32. Bellini C, Villa G, Sambuceti G, et al. Lymphoscintigraphy patterns in newborns and children with congenital lymphatic dysplasia. Lymphology 2014;47(1):28–39.
33. Mihara M, Hara H, Shibasaki J, et al. Indocyanine green lymphography and lymphaticovenous anastomosis for generalized lymphatic dysplasia with pleural effusion and ascites in neonates. Ann Vasc Surg 2015;29(6):1111–1122.
34. Wassef M, Blei F, Adams D, et al. Vascular anomalies classification: recommendations from the International Society for the Study of Vascular Anomalies. Pediatrics 2015;136(1):e203–e214.
35. Mery CM, Moffett BS, Khan MS, et al. Incidence and treatment of chylothorax after cardiac surgery in children: analysis of a large multi-institution database. J Thorac Cardiovasc Surg 2014;147(2):678–86.e1; discussion 685–686.
36. Bauman ME, Moher C, Bruce AK, Kuhle S, Kaur S, Massicotte MP. Chylothorax in children with congenital heart disease: incidence of thrombosis. Thromb Res 2013;132(2):e83–e85.
37. Savla JJ, Itkin M, Rossano JW, Dori Y. Post-operative chylothorax in patients with congenital heart disease. J Am Coll Cardiol 2017;69(19):2410–2422.
38. Lopez-Gutierrez JC, Tovar JA. Chylothorax and chylous ascites: management and pitfalls. Semin Pediatr Surg 2014;23(5):298–302.